Short communication

TiO$_2$(B) as a promising high potential negative electrode for large-size lithium-ion batteries

Minoru Inaba *, Yasuyuki Oba, Fumiharu Niina, Yosuke Murota, Yasuyuki Ogino, Akimasa Tasaka, Ken Hirota

Department of Molecular Chemistry and Biochemistry, Faculty of Science and Engineering, Doshisha University, Kyotanabe, Kyoto 610-0321, Japan

A B S T R A C T

Needle-like TiO$_2$(B) powder was obtained from K$_2$Ti$_4$O$_9$ precursor by ion exchange to protons, followed by dehydration. The charge and discharge characteristics of the TiO$_2$(B) powder were investigated as a high potential negative electrode in lithium-ion batteries. It had a high discharge capacity of 200–250 mAh g^{-1} at around 1.6 V vs. Li/Li$^+$, which was comparable with that of TiO$_2$(B) nanowires and nanotubes prepared via a hydrothermal reaction in alkaline solution. It showed very good cycleability, and gave a discharge capacity of 170 mAh g^{-1} even in the 650th cycle. It also had a high rate capability, and gave a discharge capacity of 106 mAh g^{-1} even at 10 °C.

In most of ethylene carbonate-based solutions, the TiO$_2$(B) powder exhibited good charge and discharge characteristics. However, it showed a poor compatibility with LiBF$_4$, propylene carbonate, and γ-butyrolactone. The TiO$_2$(B) powder showed good cycle performance in the presence of a non-flammable additive, trimethyl phosphate, up to 20 vol.%, and a high tolerance to water up to 1000 ppm. It was also found that inexpensive Al foil can be used as a current collector of the TiO$_2$(B) powder instead of Cu foil without sacrificing the performance.

© 2008 Elsevier B.V. All rights reserved.

1. Introduction

Recently large-size lithium-ion batteries (LIBs) have been intensively developed for use in electric vehicles and for energy storage [1]. However, there remain some problems, such as safety, durability, and cost, to be solved before commercialization of large-size LIBs.

Graphite has good properties as a negative electrode such as low operating potential (<0.25 V vs. Li/Li$^+$) and excellent cycleability [2]. On one hand, the use of the graphite negative electrode is the major ground for the advantages of LIBs: high voltage (~4 V), high energy density (~150 Wh kg^{-1} and ~400 Wh dm^{-3}), and high energy conversion efficiency in charge and discharge cycles (>95%). On the other hand, some of the safety, durability, and cost issues originate in the graphite negative electrode. For example, the formation of solid electrolyte interface (SEI) of high quality is inevitable to obtain good charge–discharge characteristics for the graphite negative electrode [2,3], which requires strict control of water content at a few tens of ppm in the electrolyte solution and the use of

expensive SEI-forming additives such as vinylene carbonate (VC) [4–6] and fluoroethylene carbonate (FEC) [4,7,8]. It is also recognized that many of safety and durability issues of LIBs are related with the damage and growth of the SEI on the graphite negative electrode.

The use of high potential negative electrodes working at potentials >1.0 V vs. Li/Li$^+$ is one of the ways for solving these safety, durability and cost issues. Though the use of high potential negative electrodes spoils some of the advantages of LIBs, such as high voltage and high energy density, the benefit to safety, durability and cost will surpass the sacrifice in voltage and energy density for use in large-size batteries. Li$_4$Ti$_5$O$_{12}$ has very flat charge and discharge curves at 1.55 V vs. Li/Li$^+$ with good cycleability [9–11], and is one of the promising candidates for high potential negative electrodes of large-size LIBs. Unfortunately the charge and discharge capacity of Li$_4$Ti$_5$O$_{12}$ is limited by the theoretical one (175 mAh g^{-1} and 607 mAh cm^{-3}), which is unfavorably lower than that of graphite (372 mAh g^{-1} and 855 mAh cm^{-3}). It has recently reported that nanowires and nanotubes of TiO$_2$(B), which are prepared via a hydrothermal reaction, have a high capacity in the range of 200–300 mAh g^{-1} at about 1.6 V vs. Li/Li$^+$ with good cycleability [12–17]. TiO$_2$(B), which is a metastable phase of titanium dioxide, has a theoretical capacity of 335 mAh g^{-1} or 1246 mAh cm^{-3},

* Corresponding author. Tel.: +81 774 65 6591; fax: +81 774 65 6841.
E-mail address: minaba@mail.doshisha.ac.jp (M. Inaba).

assuming that all Ti^{4+} ions can be reduced to Ti^{3+} as

$$TiO_2(B) + Li^+ + e^- \leftrightarrow LiTiO_2 \qquad (1)$$

The theoretical capacity is gravimetrically comparable with and volumetrically higher than that of graphite; hence, $TiO_2(B)$ is another potential candidate as a high potential negative electrode. However, the nanowires and nanotubes are prepared via a hydrothermal reaction in alkaline solution, and this raises the material cost of $TiO_2(B)$.

In the present study, a precursor, $K_2Ti_4O_9$, was prepared by a solid-state reaction, and $TiO_2(B)$ powder was obtained by ion exchange followed by dehydration [18], aiming at reducing the material cost of $TiO_2(B)$. Fundamental charge and discharge characteristics of the $TiO_2(B)$ powder were investigated as a high potential negative electrode in LIBs. Furthermore, the effects of trimethyl phosphate (TMP) as a non-flammable additive, water content in the electrolyte solutions, aluminum current collector were also studied to improve the performance and safety and to reduce the cost of batteries.

2. Experimental

$TiO_2(B)$ powder was prepared via a solid-state reaction reported by Feist and Davies [18]. K_2CO_3 (Wako Pure Chemicals, 99.8%) and anatase TiO_2 (Wako Pure Chemicals, purity: 99.9%, average diameter: 20 nm) powders were mixed in a molar ratio of 1:4, and calcined twice at 1000 °C for 24 h to obtain $K_2Ti_4O_9$ powder. The powder was washed with highly pure water and was immersed in 1.0 M HCl for 3 days to exchange the K^+ ions to protons. The resulting protonated powder was dehydrated at 500 °C for 30 min to obtain $TiO_2(B)$. The powder samples were analyzed by X-ray diffraction (XRD, Rigaku, RINT2000) and field-emission scanning electron miscroscopy (FE-SEM, JEOL, JSM7001FD).

The $TiO_2(B)$ powder was mixed with Ketjen Black (LION, EC600JD) and poly(vinyliden difluoride) (PVDF, Kureha, KF Polymer) at a weight ratio of 8:1:1, using 1-methyl-2-pyrrolidinone (Wako Pure Chemicals, reagent grade) as a solvent, to make a viscous slurry. The slurry was coated on a copper foil current collector with a surface area of 0.785 cm^2, and then dried overnight at 80 °C under vacuum. The loading of the active material was ca. 0.5 g cm^{-2}, and the thickness of the electrode layer was ca. 100 μm. In some experiments, aluminum foil was used as a current collector. Natural graphite powder (Kansai Coke and Chemicals Co., NG-7) was used as a negative electrode material for comparison. The graphite powder was mixed with PVDF at a weight ratio of 9:1, and coated on a copper foil current collector in a similar manner [4].

The electrolyte solutions used in the present study were 1.0 M LiClO$_4$ dissolved in a 1:1 mixture (by volume) of ethylene carbonate (EC) and diethyl carbonate (DEC), 1.0 M LiBF$_4$/EC + DEC (1:1), 1.0 M LiPF$_6$/EC + DEC (1:1), 1.0 M LiN(SO$_2$CF$_3$)$_2$/EC + DEC (1:1), 1.0 M LiN(SO$_2$C$_2$F$_5$)$_2$/EC + DEC (1:1), 1.0 M LiClO$_4$/propylene carbonate (PC) + DEC (1:1) and 1.0 M LiBF$_4$/γ-butyrolactone (GBL) + DEC (1:1). All these solutions were of lithium battery grade purchased from Kishida Reagent Chemicals. The water contents in these solutions were lower than 30 ppm, which were confirmed with a Karl Fischer moisture meter (Kyoto Electronics MFG, MKC-610).

The effects of trimethyl phosphate (TMP, Wako Pure Chemicals, reagent grade) were investigated as a non-flammable additive. It was added by 20 vol.% and 40 vol.% to 1.0 M LiN(SO$_2$CF$_3$)$_2$/EC + DEC (1:1), and dried over 4A molecular sieves for weeks. The solution was used for electrochemical measurements after the water content decreased below 50 ppm.

Two-electrode half cells were constructed from the $TiO_2(B)$ electrode, a separator (Celgard® 2326) and a lithium-foil counter electrode (Honjo Metal) in argon-filled glove box (Miwa, MDB-1B + MM3-P60S) with a dew point lower than −60 °C. Charge and discharge characteristics were measured at a C/6 rate between 1.0 V and 3.0 V at 30 °C, unless otherwise noted, using a battery test system (Hokuto Denko, HJ1001SM8). In the present study, lithium-ion insertion into and extraction from $TiO_2(B)$ are denoted as charging and discharging, respectively, considering the role of $TiO_2(B)$ as a negative electrode in LIBs.

3. Results and discussion

3.1. Characterization of TiO$_2$(B) powder

The formation of $TiO_2(B)$ phase after the dehydration process was confirmed by XRD analysis (JCPDS 35-0088). Unfortunately, the $TiO_2(B)$ powder was not a single phase, but contained a small amount (several percents) of the anatase phase, which was probably formed in the final dehydration process at 500 °C [18]. Fig. 1 shows an SEM image of the $TiO_2(B)$ powder. The powder has a needle-like structure with a diameter of ca. 250 nm and a length of ca. 2 μm. The shape, needle-like structure, is characteristic of the $K_2Ti_4O_9$ precursor, and did not changed appreciably after the ion exchange and dehydration processes. Hence the shape of $TiO_2(B)$ is determined in the first calcination process.

3.2. Fundamental charge and discharge characteristics in 1.0 M LiClO$_4$/EC + DEC (1:1)

Fig. 2 shows the charge and discharge curves at a C/6 rate of the $TiO_2(B)$ powder in 1.0 M LiClO$_4$ dissolved in EC + DEC (1:1). The $TiO_2(B)$ powder showed a sloping plateau at ca. 1.6 V on the charge and discharge curves, which are similar to those reported for $TiO_2(B)$ nanowires and nanotubes [12–17]. The initial discharge capacity was 246 mAh g^{-1}, which is higher than that of Li$_4$Ti$_5$O$_{12}$ [9–11] and comparable with that of $TiO_2(B)$ nanowires and nanotubes [12–17]. A considerably high irreversible capacity (123 mAh g^{-1}) was observed in the first cycle, but disappeared in the second and the subsequent cycles. Lower discharge rates did not appreciably decrease the irreversible capacity; hence, the high irreversible capacity is not due to a slow kinetics of the reaction. In contrast, when the lower potential limit was set at 1.4 V (not shown), the irreversible capacity decreased greatly to ca. 40 mAh g^{-1}. Hence the high irreversible capacity most probably
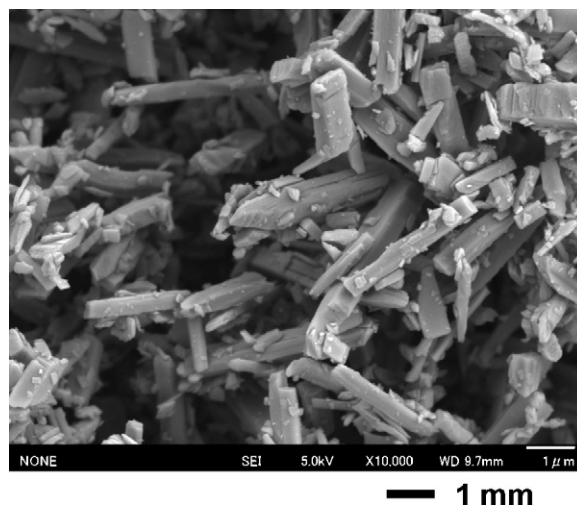

Fig. 1. SEM image of TiO$_2$(B) powder prepared from K$_2$Ti$_4$O$_9$ precursor by ion exchange and dehydration.
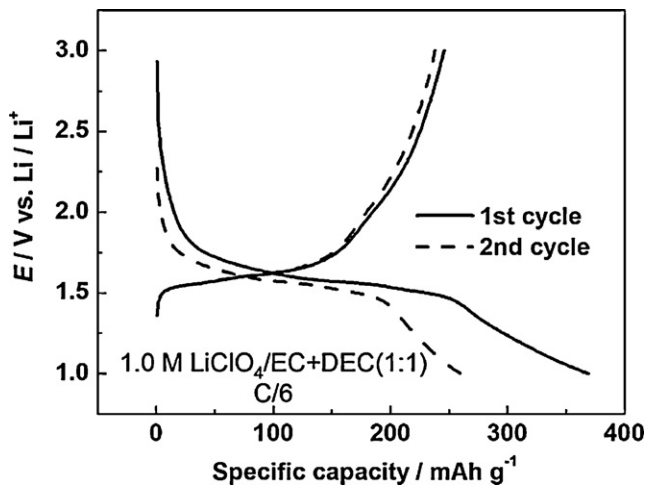
Fig. 2. Charge/discharge curves of TiO$_2$(B) at C/6 in 1 M LiClO$_4$/EC + DEC (1:1).

originated from surface reactions, such as solvent decomposition, at potentials <1.4 V.

The cycleability at C/6 and rate capability of the TiO$_2$(B) powder is shown in Fig. 3. The TiO$_2$(B) powder exhibited very good cycleability. After an initial drop in discharge capacity, high dis-
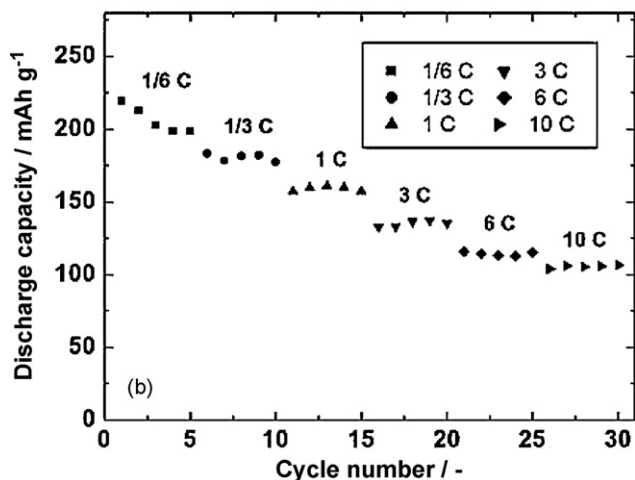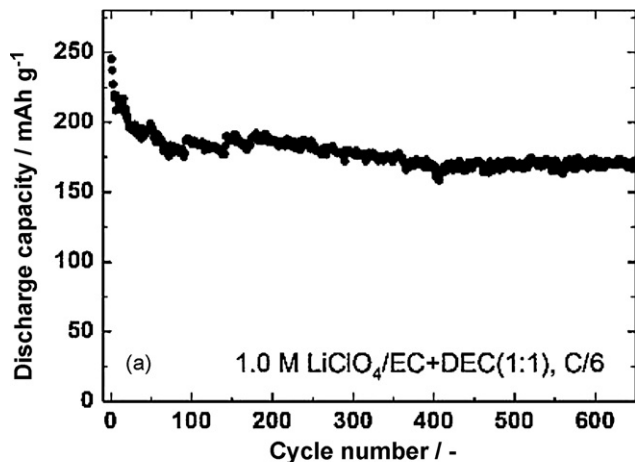

Fig. 3. Cycleability at C/6 (a) and rate capability (b) of TiO$_2$(B) in 1 M LiClO$_4$/EC + DEC (1:1). The charge rate was equivalent to the discharge rate for rate capability measurements.

charge capacities of ca. 200 mAh g^{-1} with Coulombic efficiencies close to 100% were stably obtained. The discharge capacity as high as 170 mAh g^{-1} was obtained even in the 650th cycle. The good cycleability indicates a high structural integrity of TiO$_2$(B), though TiO$_2$(B) is a metastable phase. The TiO$_2$(B) powder showed a high rate capability as well. Even at a high rate of 10 C, it gave a discharge capacity of 106 mAh g^{-1}, which is about a half of that obtained at low rates. TiO$_2$(B) is an insulator, but the insertion of Li$^+$ ions on charging produces Ti^{3+} ions in the lattice, and gives a good electronic conductivity. The high rate capability probably originates from the good electronic conductivity by the formation of Ti^{3+}, which is similar to Li$_4$Ti$_5$O$_{12}$. The results in Figs. 2 and 3 revealed that the TiO$_2$(B) powder is very promising as a high potential negative electrode material in large-size LIBs with high capacity, good cycleability, high rate capability, and low cost.

3.3. Charge and discharge characteristics in different electrolyte systems

The charge and discharge characteristics of TiO$_2$(B) at C/6 in different electrolyte solutions are summarized in Fig. 4. TiO$_2$(B) showed good cycleability with a high discharge capacity of ca. 200 mAh g^{-1} in most of the EC-based electrolyte solutions. The charge and discharge curves in 1.0 M LiPF$_6$/EC + DEC (1:1) are shown in Fig. 5. The irreversible capacity in 1.0 M LiPF$_6$/EC + DEC (1:1) was much lower (43 mAh g^{-1}) than that in 1.0 M LiClO$_4$/EC + DEC (1:1) shown in Fig. 2. Similar results were obtained in 1.0 M LiN(SO$_2$CF$_3$)$_2$/EC + DEC (1:1) and 1.0 M LiN(SO$_2$C$_2$F$_5$)$_2$/EC + DEC (1:1), though these solutions gave slightly higher irreversible capacities (65 mAh g^{-1} and 67 mAh g^{-1}, respectively) than 1.0 M LiPF$_6$/EC + DEC (1:1). The lower irreversible capacities were obtained in these solutions, probably because the fluorine-containing electrolyte salts (LiPF$_6$, LiN(SO$_2$CF$_3$)$_2$, and LiN(SO$_2$C$_2$F$_5$)$_2$) suppress surface reactions such as solvent decomposition at potentials <1.4 V.

In contrast, LiBF$_4$ electrolyte salt gave a low discharge capacity, and PC and GBL solvents gave poor cycleability as shown in Fig. 4. The use of PC and GBL instead of EC as a primary solvent is attractive because they would improve the charge and discharge characteristics at low temperatures [4]. In these solutions, the initial discharge capacity was high (ca. 200 mAh g^{-1}), but the capacity decreased gradually in PC + DEC (1:1) and rapidly in GBL + DEC (1:1). Postmortem analysis revealed that many cracks and bulges were formed on the electrode surface after cycled in these solutions. Therefore
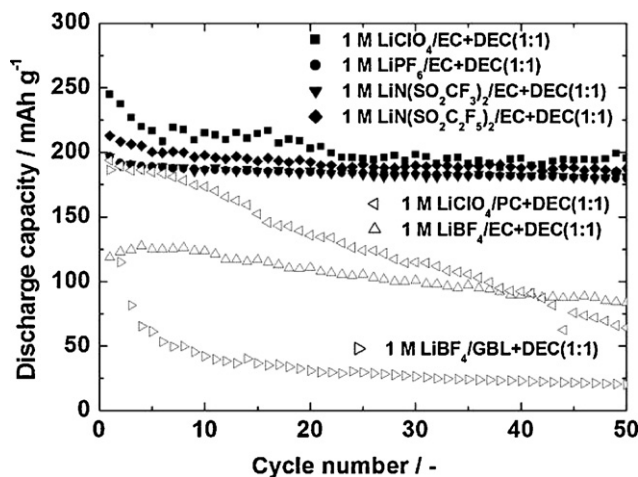

Fig. 4. Variations of discharge capacity of TiO$_2$(B) at C/6 with cycle number in different electrolyte solutions.

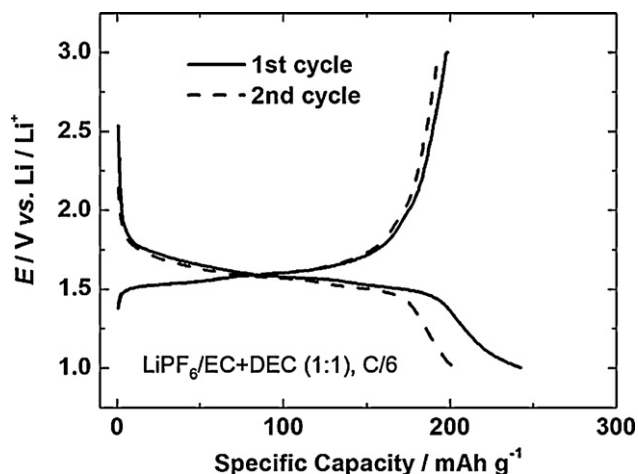**Fig. 5.** Charge/discharge curves of $TiO_2(B)$ at C/6 in 1 M $LiPF_6/EC + DEC$ (1:1).

Fig. 7. Effects of a non-flammable additive, TMP, on the charge and discharge characteristics of $TiO_2(B)$ in $LiN(SO_2C_2F_5)_2/EC + DEC$ (1:1). Charge and discharge rate: C/6.

the poor cycleability in PC + DEC and GBL + DEC is closely related with solvent decomposition and excessive surface film formation. Effective additives are needed to suppress solvent decomposition in these solvents.

It is widely recognized that graphite negative electrode is very sensitive to water [2], by which we use highly purified electrolyte solutions with a very low water content (usually lower than a few tens of ppm) for LIBs. The effects of water on the charge and discharge characteristics of $TiO_2(B)$ and graphite (NG7) are shown in Fig. 6. Here we used $LiN(SO_2C_2F_5)_2$ to avoid the hydrolysis of electrolyte salts. The graphite negative electrode exhibited a high capacity of ca. 370 mAh g^{-1} in the initial cycle, which is very close to the theoretical capacity (372 mAh g^{-1}). At a low water content (10 ppm), it showed good cycleability; however, the capacity decreased significantly with cycle number at a water content of 100 ppm. In contrast, $TiO_2(B)$ exhibited a very high tolerance to water. As shown in Fig. 6, the cycleability of $TiO_2(B)$ did not change appreciably even at a water content of 1000 ppm. This high tolerance to water of $TiO_2(B)$ is one of advantages over graphite, and may greatly reduce the purification cost of solvent.

Safety is one of the important issues in large-size LIBs. Non-flammable electrolyte solutions are attractive to improve the safety
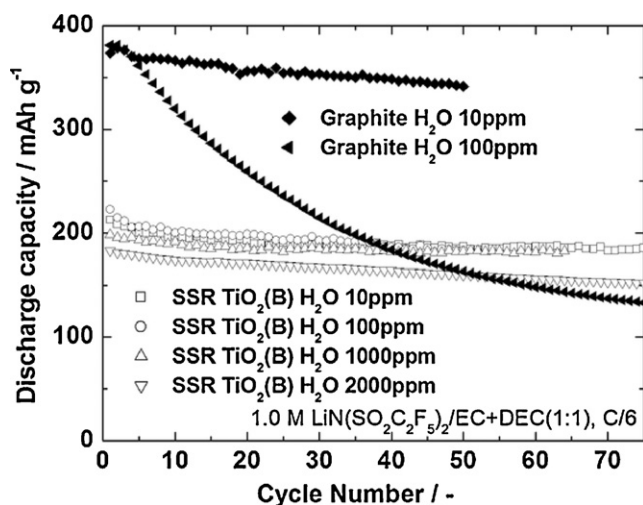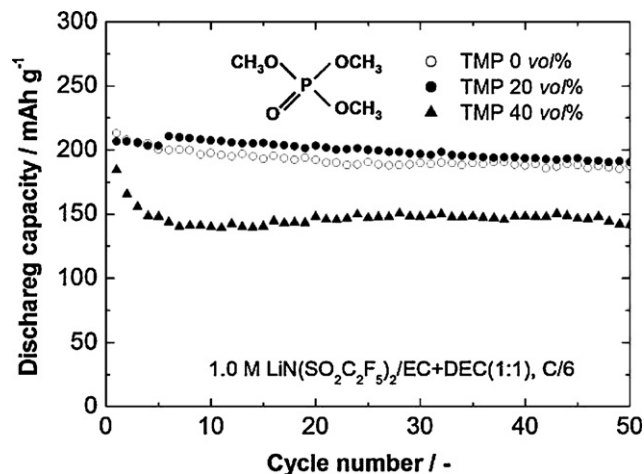
of LIBs. It has been reported that TMP is effective as a non-flammable additive [19–21]. For example, in the case of EC + DEC (1:1) solvent systems, 20 vol.% addition of TMP makes the solvent self-extinguishable, and 30 vol.% addition non-flammable [21]. Unfortunately TMP has poor compatibility with graphite negative

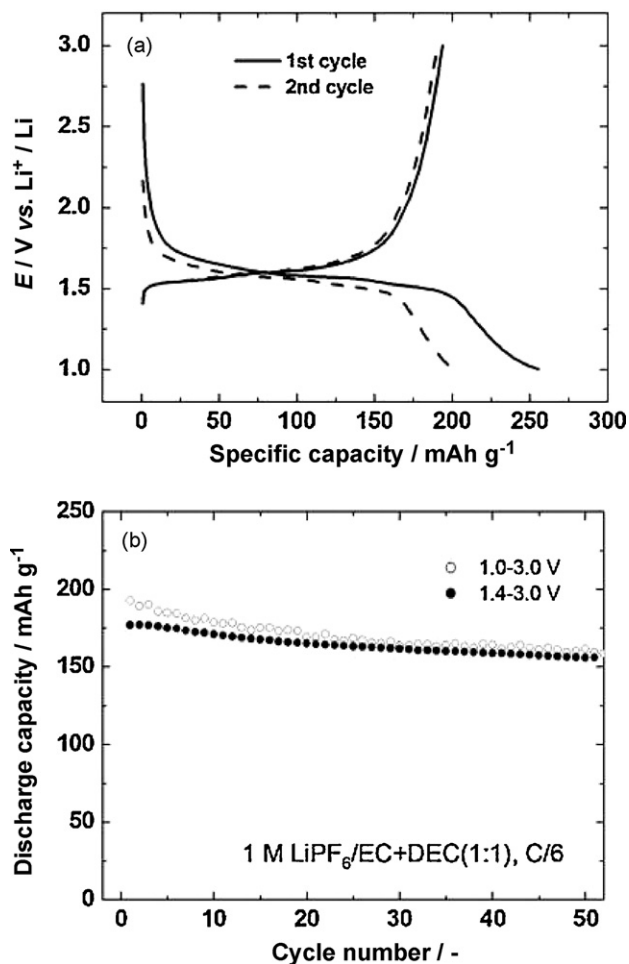**Fig. 8.** Charge and discharge curves (a) and cycleability (b) of $TiO_2(B)$ coated on Al current collector in 1 M $LiPF_6/EC + DEC$ (1:1). Charge and discharge rate: C/6.

Fig. 6. Effects of water content on the charge and discharge characteristics of natural graphite (NG7) and $TiO_2(B)$ negative electrodes in 1.0 M $LiN(SO_2C_2F_5)_2/EC + DEC$ (1:1). Charge and discharge rate: C/6.

electrode, because of instability of TMP at potentials <1.0 V [19]. Fig. 7 shows the effects of TMP on the charge and discharge characteristics of $TiO_2(B)$ in 1.0 M $LiN(SO_2C_2F_5)_2$/EC + DEC (1:1). The addition of TMP up to 20 vol.% (self-extinguishable) did not change appreciably the cycleability of $TiO_2(B)$. The addition of 40 vol.% TMP decreased the capacity to ca. 150 mAh g^{-1} in the several initial cycles; however, the cycleability was fairly good in the following cycles up to the 50th cycle. It is hence concluded that $TiO_2(B)$ has a good compatibility with TMP, which enables us to produce large-size LIBs with improved safety.

3.4. Effects of aluminum current collector

The prices of metals, not only precious metals, but also base metals, have been increasing lately, which is now a serious problem in the cost of LIBs, especially of large-size ones. Copper, which is exclusively used as a current collector for graphite negative electrode in LIBs, is one of such price-rising base metals (<$1.0/lb in 2003 to $3.7/lb in July 2008) [22]. Aluminum is much less expensive than copper, but cannot be used as a current collector for graphite negative electrode because Li–Al alloy is formed at around 0.5 V vs. Li/Li$^+$. However, the use of high potential negative electrodes working at potentials >1.0 V may allow the use of aluminum as a current collector. Fig. 8 shows charge and discharge characteristics of $TiO_2(B)$ coated on an Al current collector in 1.0 M $LiPF_6$/EC + DEC(1:1). As was expected, $TiO_2(B)$ showed good charge and discharge characteristics on the Al current collector. The initial discharge capacity was 194 mAh g^{-1} with a good cycleability, which is comparable with that obtained on the Cu current collector shown in Fig. 5. These preliminary data are encouraging in reducing the cost of LIBs, though cycleability in much more extended cycles should be investigated for practical use.

4. Conclusions

A precursor, $K_2Ti_4O_9$, was prepared by a solid-state reaction, and $TiO_2(B)$ powder was obtained by ion exchange to protons, followed by dehydration. The $TiO_2(B)$ powder, which has a needle-like structure, showed a high discharge capacity of 200–250 mAh g^{-1} at around 1.6 V vs. Li/Li$^+$. The discharge capacity was higher than that of $Li_4Ti_5O_{12}$ and was comparable with that of $TiO_2(B)$ nanowires and nanotubes prepared via a hydrothermal reaction in alkaline solution. It showed very good cycleability, and gave a discharge capacity of 170 mAh g^{-1} even in the 650th cycle. It also showed a high rate capability, and gave a discharge capacity of 106 mAh g^{-1} even at a high rate of 10 C. These results indicated that the $TiO_2(B)$ powder is very promising as a high potential negative electrode material in large-size lithium-ion batteries with high capacity, good cycleability, high rate capability, and low cost.

The charge and discharge characteristics of the $TiO_2(B)$ powder were investigated in different electrolyte systems. In most of EC-based solutions, the $TiO_2(B)$ powder exhibited good charge and discharge characteristics. However, it showed a poor compatibility with $LiBF_4$, PC, and GBL. It was considered that the poor compatibility is due to solvent decomposition and excessive surface film formation in these electrolyte solutions. The $TiO_2(B)$ powder showed good cycle performance in the presence of a non-flammable additive, TMP, up to 20 vol.%, and showed a high tolerance to water up to 1000 ppm. It was also found that inexpensive aluminum foil can be used as a current collector of the $TiO_2(B)$ powder instead of copper foil without sacrificing the performance.

The discharge capacity (200–250 mAh g^{-1}) of $TiO_2(B)$ obtained in the present study was higher than that of $Li_4Ti_5O_{12}$, but was considerably lower than the theoretical capacity of $TiO_2(B)$ (335 mAh g^{-1}). The reason is not clear at present, and our next goal is to improve the reversible capacity as high as possible.

Acknowledgment

References

[1] B. Scrosati, Nature 373 (1995) 557.
[2] Z. Ogumi, M. Inaba, Bull. Chem. Soc. Jpn. 71 (1998) 521.
[3] S.S. Zhang, J. Power Sources 162 (2006) 1379.
[4] S.-K. Jeong, M. Inaba, R. Mogi, Y. Iriyama, T. Abe, Z. Ogumi, Langmuir 17 (2001) 8281.
[5] B. Simon, J.P. Boeuve, US Patent 5,626,981 (1997).
[6] T. Sasaki, T. Abe, Y. Iriyama, M. Inaba, Z. Ogumi, J. Electrochem. Soc. 152 (2005) A2046.
[7] R. Mogi, M. Inaba, S.K. Jeong, Y. Iriyama, T. Abe, Z. Ogumia, J. Electrochem. Soc. 149 (2002) A1578.
[8] R. McMillan, H. Slegr, Z.X. Shu, W.D. Wang, J. Power Sources 81–82 (1999) 20.
[9] T. Ohzuku, A. Ueda, N. Yamamoto, J. Electrochem. Soc. 142 (1995) 1431.
[10] K.M. Colbow, J.R. Dahn, R.R. Haering, J. Power Sources 26 (1989) 397.
[11] K. Zaghib, M. Simoneau, M. Armand, M. Gauthier, J. Power Sources 81–82 (1999) 300.
[12] G. Armstrong, A.R. Armstrong, J. Canales, P.G. Bruce, Electrochem. Solid State Lett. 9 (2006) A139.
[13] A.R. Armstrong, G. Armstrong, J. Canales, P.G. Bruce, Angew. Chem. Int. Ed. 43 (2004) 2286.
[14] A.R. Armstrong, G. Armstrong, J. Canales, P.G. Bruce, J. Power Sources 146 (2005) 501.
[15] A.R. Armstrong, G. Armstrong, J. Canales, R. García, P.G. Bruce, Adv. Mater. 17 (2005) 862.
[16] H. Zhang, G.R. Li, L.P. An, T.Y. Yan, X.P. Gao, H.Y. Zhu, J. Phys. Chem. C 111 (2007) 6143.
[17] L.P. An, X.P. Gao, G.R. Li, T.Y. Yana, H.Y. Zhub, P.W. Shen, Electrochim. Acta 53 (2008) 4573.
[18] T.P. Feist, P.K. Davies, J. Solid State Chem. 101 (1992) 275.
[19] X. Wang, E. Yasukawa, S. Kasuya, J. Electrochem. Soc. 148 (2001) A1058.
[20] X. Wang, E. Yasukawa, S. Kasuya, J. Electrochem. Soc. 148 (2001) A1066.
[21] M. Morita, Y. Niida, N. Yoshimoto, K. Adachi, J. Power Sources 146 (2005) 427.
[22] Kitco Inc. Homepage. http://www.kitconet.com/.